Biogeosciences Discuss., 9, 15787–15821, 2012
www.biogeosciences-discuss.net/9/15787/2012/
doi:10.5194/bgd-9-15787-2012

Biogeosciences
Discussions

# Kinetic bottlenecks to chemical exchange rates for deep-sea animals II: Carbon dioxide

**A. F. Hofmann[1,2], E. T. Peltzer[1], and P. G. Brewer[1]**

[1]Monterey Bay Aquarium Research Institute (MBARI), 7700 Sandholdt Road, Moss Landing, CA 95039–9644, USA
[2]current address: German Aerospace Center (DLR), Institute of Technical Thermodynamics, Pfaffenwaldring 38–40, 70569 Stuttgart, Germany

Received: 4 October 2012 – Accepted: 28 October 2012 – Published: 9 November 2012

Correspondence to: A. F. Hofmann (ahofmann.mbari@gmail.com)

Published by Copernicus Publications on behalf of the European Geosciences Union.

## Abstract

Increased ocean acidification from fossil fuel $CO_2$ invasion, from temperature-driven changes in respiration, and from possible leakage from sub-seabed geologic $CO_2$ disposal has aroused concern over the impacts of elevated $CO_2$ concentrations on marine life. Discussion of these impacts has so far focused only on changes in the oceanic bulk fluid properties ($\Delta$pH, $\Delta[\sum CO_2]$ etc.) as the critical variable and with a major focus on carbonate shell dissolution. Here we describe the rate problem for animals that must export $CO_2$ at about the same rate at which $O_2$ is consumed. We analyze the basic properties controlling $CO_2$ export within the diffusive boundary layer around marine animals in an ocean changing in temperature ($T$) and $CO_2$ concentration in order to compare the challenges posed by $O_2$ uptake under stress with the equivalent problem of $CO_2$ expulsion. The problem is more complex than that for a non-reactive gas since, as with gas exchange of $CO_2$ at the air-sea interface, the influence of the ensemble of reactions within the $CO_2$-$HCO_3^-$-$CO_3^{2-}$ acid-base system needs to be considered. These reactions significantly facilitate $CO_2$ efflux compared to $O_2$ intake at equal temperature, pressure and flow rate under typical oceanic concentrations.The effect of these reactions can be described by an enhancement factor. For organisms, this means mechanically increasing flow over their surface to thin the boundary layer as is required to alleviate $O_2$ stress seems not necessary to facilitate $CO_2$ efflux. Nevertheless the elevated $pCO_2$ cost most likely is non-zero. Regionally as with $O_2$ the combination of $T$, $P$, and pH/$pCO_2$ creates a zone of maximum $CO_2$ stress at around 1000 m depth. But the net result is that, for the problem of gas exchange with the bulk ocean, the combination of an increasing $T$ combined with declining $O_2$ poses a greater challenge to marine life than does increasing $CO_2$. The relationships developed here allow a more accurate prediction of the impacts on marine life from the combined effects of changing $T$, $O_2$, and $CO_2$ than can be estimated from single variable studies.

Title Page
Abstract | Introduction
Conclusions | References
Tables | Figures
◀| |▶
◀ ▶
Back | Close
Full Screen / Esc
Printer-friendly Version
Interactive Discussion

## 1 Introduction

Modern climate change concerns over ocean chemical impacts arise from two primary issues: metabolic/respiratory stress imposed by rising temperature and the inevitably associated decline in dissolved $O_2$ (Shaffer et al., 2009), and the impacts of ocean acidification on both calcification and the more general systemic metabolic stress (Caldeira et al., 2005). In a companion paper (Hofmann et al., 2012) we addressed the problem of changing $T$ and $O_2$ in terms of gas uptake rates across the animal respiratory surface diffusive boundary layer for typical oceanic profiles with depth. Here we describe the related problem for the required $CO_2$ export that must over time match the equivalent $O_2$ import.

The rise in concern over ocean acidification from the invasion of fossil fuel $CO_2$ (e.g., Caldeira and Wickett, 2003, 2005; Royal Society, 2005; Blackford and Gilbert, 2007; Meehl et al., 2007; IPCC, 2007; Zeebe et al., 2008) has lead to increased attention to the potential impact of elevated ocean $CO_2$ levels on marine animals. The early plans for direct ocean $CO_2$ sequestration, first advocated by Marchetti (1977), as a means of mitigating the impacts of climate change drew little attention. But as plans for experimental testing of this scheme at a site off Hawaii surfaced opposition soon arose (Haugan, 2003). The first expressions of this from the general public were unspecific and the scientific community soon realized that far too little authoritative information was available (Kita and Ohsumi, 2004). The early laboratory experiments that were carried out showed impacts of elevated $CO_2$ (low pH) on calcification in marine species (Gattuso et al., 1998), and potential coralline impacts are today a major field of scientific study (Orr et al., 2005).

The first small-scale experimental field test of true deep-sea $CO_2$ injection (Brewer et al., 1999) aroused great interest and was important in resolving numerous complex physicochemical issues such as the role of hydrate formation and the lifetime and fluid dynamics of the material. Images of a deep-sea fish swimming within a few centimeters of the released liquid $CO_2$ drew attention, and general concerns over possible sublethal stress on deep-sea animals quickly became a matter of debate.

Seibel and Walsh (2001, 2003) reviewed the existing literature and inferred that impaired physiological performance would occur for many deep-sea animals under elevated $CO_2$ levels and noted in particular that “oxygen transport proteins are highly sensitive to changes in pH”. The matter of deep-sea $CO_2$ injection was carefully evaluated in a major IPCC report (Caldeira et al., 2005) and the concern that deep-sea animals “would experience serious problems in oxygen supply under conditions of increased $CO_2$ concentrations” was reiterated; but a numerical framework within which to address this was not reported. The possible linkage between $O_2$ and $CO_2$ impacts on the functioning of marine animals remains to be formally addressed.

The challenge today is to find ways to combine the effects of simultaneous changes in $T$, $O_2$, and $CO_2$ within the same conceptual and numerical framework so that more quantitative estimates of impacts can be made. The result of long term changes in the ocean’s oxygen status under global warming have been modeled by Shaffer et al. (2009) who concluded that the suboxic ($\leq 10\,\mu\text{mol}\,O_2\,\text{kg}^{-1}$) and hypoxic ($\leq 80\,\mu\text{mol}\,\text{kg}^{-1}$) oceanic regions would greatly expand. The long term evolution of the coupled atmospheric and oceanic thermal and $CO_2$ signals under various scenarios has been extensively modeled (e.g., Sarmiento and Toggweiler, 1984; Siegenthaler and Wenk, 1984; Sarmiento et al., 1995; Archer et al., 1998; Archer, 1999; Sabine et al., 2004; Archer, 2005; IPCC, 2007; Archer et al., 2009; Allen et al., 2009; Allison et al., 2009). But the impact of these combined effects on marine life remains uncertain.

Here we analyze the physical limits that apply, and by the use of simple physical and thermodynamic relationships we shed important light on the differing thermodynamic efficiencies of the mechanisms and routes taken by the $O_2$ and $CO_2$ molecules as they exchange in the boundary between the animal and the bulk fluid. In order to minimize respiratory acidosis and associated detrimental effects (e.g., Perry et al., 2010) as a result of $CO_2$ build-up inside an animal it is obvious that $CO_2$ must be exported from the cell to keep the respiration reaction energetically favorable and efficient. To maintain mass balance, the rate of $CO_2$ export must be stoichiometrically related to $O_2$ consumption. By analyzing the process by which $CO_2$ is transferred from the outer membrane through the diffusive boundary layer to the bulk ocean it is possible to better evaluate the relative impacts of $O_2$ and $CO_2$ stress and more accurately predict the impacts of climate-ocean $CO_2$ changes on marine life.

In this paper, we investigate the diffusive limitation of $CO_2$ export as compared to the equivalent diffusive limitation of $O_2$ uptake, which we have reported in a companion paper Hofmann et al. (2012).

It is important to note that we are not addressing here the internal impacts on animal chemical functioning. We simply ask the question of whether, when faced with external $CO_2$ levels that could impair function, the animal must resort to increasing physical flow over the surface, or whether the same boundary layer thickness required for $O_2$ import is still sufficient to support the equivalent, ocean chemistry enhanced, $CO_2$ export.

## 2 Materials and methods

### 2.1 The oceanic $CO_2$ removal potential $RP_{CO_2}$

### 2.1.1 Boundary layer $CO_2$ diffusion with no reaction

As a first order approximation, the $CO_2$ efflux from an organism that consumes oxygen at a rate of $E^{O_2}$ (in $\mu mol\, s^{-1}\, cm^{-2}$) can be defined as

$$E^{CO_2} = E^{O_2} \tag{1}$$

with the directions of the fluxes being opposite to each other.

We treat diffusion and $CO_2$ reactivity in seawater in two separate steps. First, we assume no $CO_2$ reactivity in seawater, and consider only the theoretical, purely diffusive $CO_2$ export flux: $E^{CO_2}_{diff}$. Following the same reasoning as in the companion paper (Hofmann et al., 2012) treating diffusive $O_2$ uptake limitations, we consider a step-wise process of diffusion through the respiratory tissue and the diffusive boundary layer (DBL) in contact with this tissue. We define a transfer time for each step and, by taking the inverse of these times, define a term for the total diffusion-only $CO_2$ export flux (in $\mu mol\,s^{-1}\,cm^{-2}$) from the organism as

$$E_{\text{diff}}^{CO_2} = 1 \Bigg/ \left( \frac{1}{E_{\text{diff, DBL}}^{CO_2}} + \frac{1}{E_{\text{diff, tissue}}^{CO_2}} \right) \tag{2}$$

with

$$E_{\text{diff, DBL}}^{CO_2} = \frac{D^{CO_2}\,\rho_{SW}}{L^{CO_2}\,K0'^{CO_2}}\,\Delta pCO_2|_{\text{DBL}} \tag{3}$$

where $\rho_{SW}$ is the in situ density of seawater (calculated according to Millero and Poisson, 1981, as implemented in Hofmann et al., 2010) in $kg\,cm^{-3}$, and where $K0'^{CO_2}$ is the apparent Henry's constant for $CO_2$ in $mol\,kg^{-1}\,atm^{-1}$ (= $\mu mol\,kg^{-1}\,\mu atm^{-1}$) at in-situ conditions

$$K0'^{CO_2} = \frac{[CO_2]}{pCO_2([CO_2], T, S, P)} \tag{4}$$

$[CO_2]$ in $mol\,kg^{-1}$ here is an arbitrary concentration and in the denominator $pCO_2$ in atm is first calculated in the conventional way from $[CO_2]$ using the common mass unit Henry's constant $K0$, calculated according to Weiss (1974) using potential temperature ($\theta$, Bryden, 1973; Fofonoff, 1977), and the fugacity coefficient for $CO_2$ calculated as given in Zeebe and Wolf-Gladrow (2001) (restated from Koertzinger, 1999). Resulting $pCO_2$ values are then corrected for hydrostatic pressure (calculated from given depth values according to Fofonoff and Millard, 1983) according to Enns et al. (1965).

Again, as in (Hofmann et al., 2012), we now consider the external physical constraints on respiratory gas exchange imposed by the surrounding ocean, which means

$E^{CO_2}_{tissue} >> E^{CO_2}_{DBL}$. This implies that the total flux $E^{CO_2}_{diff}$ approaches $E^{CO_2}_{DBL}$ and Eq. (2) can be restated as

$$E^{CO_2}_{diff} \le \frac{D^{CO_2}\,\rho_{SW}}{L^{CO_2}\,K0'^{CO_2}}\,\Delta pCO_2|_{DBL} \tag{5}$$

### 2.1.2 Boundary layer $CO_2$ reactivity: the enhancement factor EF

In contrast to the $O_2$ case, $CO_2$ is reactive in seawater via acid-base equilibration reactions of the carbonate system (e.g., Zeebe and Wolf-Gladrow, 2001), the most important ones being

$$CO_2 + H_2O \longleftrightarrow HCO_3^- + H^+ \tag{6}$$

$$CO_2 + OH^- \longleftrightarrow HCO_3^- \tag{7}$$

While these reactions and other aquatic acid-base equilibration reactions can be treated in great detail (e.g., Hofmann et al., 2008, 2010), very reasonable approximations (Emerson, 1975; Zeebe and Wolf-Gladrow, 2001) give a dimensionless "enhancement factor" EF that well describes the enhancement of diffusive $CO_2$ transport by the above reactions

$$EF = \frac{E^{CO_2}}{E^{CO_2}_{diff}} = f(L^{CO_2}, T, S, P, pH_{free\ scale}) \tag{8}$$

where $E^{CO_2}$ represents the true $CO_2$ flux including the effect of chemical reactions and $E^{diff}_{CO_2}$ is the hypothetical diffusive flux that would occur if $CO_2$ were not chemically reactive in seawater, as described in Sect. 2.1.1. The dimensionless factor EF is a function of the thickness of the diffusive boundary layer for $CO_2$, $L^{CO_2}$ in cm, temperature $T$ in °C, salinity $S$, hydrostatic pressure $P$ in bar, and the ambient pH on the free scale $pH_{\text{free scale}}$. It can be calculated for plane geometry, which is here used as a first order approximation for any biologic gas exchange surface, as

$$\text{EF} = \frac{L^{CO_2}}{a_k} \coth\left(\frac{L^{CO_2}}{a_k}\right) \tag{9}$$

with = $a_k$ in cm being the reacto-diffusive length scale for $CO_2$ diffusion and the reactions given in Eqs. (6) and (7), which can be calculated as

$$a_k = \sqrt{\frac{D^{CO_2}}{k_{+1} + k_{+4}\,[OH^-]}} \tag{10}$$

Again, the molecular diffusion coefficient for $CO_2$ in $cm^2\,s^{-1}$, $D^{CO_2}$, can be calculated as a function of $S$, $T$, and $P$. $k_{+1}$ is the forward rate constant in $s^{-1}$ of the reaction of $CO_2$ and $H_2O$ (Eq. 6) and $k_{+4}$ is the forward rate constant in $kg\,mol^{-1}\,s^{-1}$ of the reaction of $CO_2$ and $OH^-$ (Eq. 7), both can be calculated ($k_{+1}$ and $k_{+4}$ are here calculated as given in Zeebe and Wolf-Gladrow (2001) as functions of temperature $T$. $[OH^-]$ is the hydroxyl ion concentration in $mol\,kg^{-1}$ calculated as

$$[OH^-] = \frac{K_W}{10^{-pH_{\text{free scale}}}\,\frac{mol}{kg}} \tag{11}$$

where $K_W$ in $mol^2\,kg^{-2}$ is the ion product of water, calculated ($K_W$ is here calculated after Millero (1995) as implemented in Hofmann et al. (2010)) as a function of temperature $T$ and salinity $S$.

Note that Zeebe and Wolf-Gladrow (2001) also define a "spherical" version of EF which is meant for microorganisms where the effective thickness of the DBL (i.e., $L^{CO_2}$

here) is equal to the radius of the sphere (e.g., Zeebe and Wolf-Gladrow, 2001). While being a valuable description for plankton and unicellular algae, for any other (i.e., macroscopic) organism, the planar description is more appropriate: while there will be a specific description for each animal shape, gas exchange tissue shape and size, mode of swimming and pumping etc., there will always be a dependency on the flow velocity across the gas exchange tissue. The planar surface description is the most generic and widely applicable description that allows for such a parameterization. It is also given in this form in Zeebe and Wolf-Gladrow (2001), and therefore we use it here.

Using EF we can write an equation for the $CO_2$ export flux from an organism (in $\mu mol\,s^{-1}\,cm^{-2}$), considering both diffusion and $CO_2$ reactivity in seawater

$$E^{CO_2} = E_{diff}^{CO_2}\,EF \tag{12}$$

Using Eq. (2), for $E_{diff}^{CO_2}$, this means

$$E^{CO_2} \leq \frac{D^{CO_2}\,\rho_{SW}\,K0'^{CO_2}\,EF}{L^{CO_2}}\,\Delta pCO_2|_{DBL} \tag{13}$$

### 2.1.3 Defining $RP_{CO_2}$ equivalently to $SP_{O_2}$

In order to define a quantity similar to the oceanic oxygen supply potential $SP_{O_2}$ in the oxygen companion paper (Hofmann et al., 2012), we now divide both sides of the equation by the DBL thickness $L^{CO_2}$ (For $O_2$ this results in a purely oceanic property that is independent of any animal specific boundary layer thickness; however the chemical reactivity of the $CO_2$ molecule within the boundary layer prohibits such simplification here although we show that a close approximation is possible).

$$E^{CO_2}\,L^{CO_2} \leq D^{CO_2}\,\rho_{SW}\,K0'^{CO_2}\,EF\,\Delta pCO_2|_{DBL} \tag{14}$$

Considering the limiting case, i.e., the maximal upper boundary for the $CO_2$ removal rate, we can now define the oceanic $CO_2$ removal potential (in $\mu mol\, s^{-1}\, cm^{-1}$) as

$$\mathrm{RP}_{CO_2} := D^{CO_2}\, \rho_{SW}\, K0'^{CO_2}\, \mathrm{EF}\, \Delta p\mathrm{CO}_2|_{\mathrm{DBL}} \tag{15}$$

However, as opposed to the $O_2$ case, where $\mathrm{SP}_{O_2}$ is independent of the description of the DBL used, i.e., the DBL thickness $L$, here, EF is a function of $L^{CO_2}$, which means $\mathrm{RP}_{CO_2}$ depends on a model description for the DBL. Again, we use a generic planar surface description as given in Table 1 (adapted for $CO_2$ from Hofmann et al. (2012)).

While the term $\mathrm{RP}_{CO_2}$ itself does depend on the DBL properties, $\mathrm{RP}_{CO_2}$ with $\mathrm{EF} = 1$ can be interpreted as a "purely diffusive" oceanic $CO_2$ removal potential, a quantity that is not dependent on a DBL model description. The more realistic quantity with real physico-chemical meaning, however, is $\mathrm{RP}_{CO_2}$ with EF as calculated above in Eq. (9). We point out that the boundary layer property $L^{CO_2}$-description here (as well as the planar EF description) is meant for large scale oceanic comparison only and appropriate values can and should be substituted for organism and system specific descriptions if this is desired. The sensitivity of our calculations with respect to fluid flow velocities are explored below.

$\mathrm{RP}_{CO_2}$ depends on the $CO_2$ partial pressure differential $\Delta p\mathrm{CO}_2|_{\mathrm{DBL}} = \left(p\mathrm{CO}_2|_s - p\mathrm{CO}_2|_f\right)$ across the DBL with $p\mathrm{CO}_2|_f$ being the ambient free stream $p\mathrm{CO}_2$ value and $p\mathrm{CO}_2|_s$ being the $p\mathrm{CO}_2$ value directly at the organism surface. Here, we investigate outer envelopes of diffusive $CO_2$ export limitations, i.e., we are interested in maximal values for $\mathrm{RP}_{CO_2}$. $\Delta p\mathrm{CO}_2|_{\mathrm{DBL}}$ and thus $\mathrm{RP}_{CO_2}$ are maximal when $p\mathrm{CO}_2|_s$ is maximal.

### 2.1.4 $p\mathrm{CO}_2|_s^{\max}$, an exemplary maximal value for the $CO_2$ partial pressure in molecular contact with an organism

The sensitivity of marine animals to elevated internal $p\mathrm{CO}_2$ levels varies with species and life stage. Absolute limits are hard to define, as knowledge about the effects of

Title Page
Abstract Introduction
Conclusions References
Tables Figures
|◀ ▶|
◀ ▶
Back Close
Full Screen / Esc
Printer-friendly Version
Interactive Discussion

acute hypercapnia is still limited (see, e.g., Caldeira et al., 2005; Poertner et al., 2005). Almost nothing is know about the limits for $p\mathrm{CO_2}$ or pH in diffusive molecular contact with the outside of the gas exchange surface of an organism. However, to calculate maximal $\mathrm{RP_{CO_2}}$ values, Eq. (15) requires a maximal value for $p\mathrm{CO_2}|_\mathrm{s}$, which exactly represents this maximal $p\mathrm{CO_2}$ directly at the (gas exchange) surface of an organism. For the example calculations given here, comparing various oceanic regions amongst each other, we use one single, constant value $p\mathrm{CO_2}|_\mathrm{s} = p\mathrm{CO_2}|_\mathrm{s}^\mathrm{max} = 5000\,\mu\mathrm{atm}$. If attained in the external medium, this $p\mathrm{CO_2}$ would produce effects such as narcosis and mortality in sensitive organisms (Caldeira et al., 2005).

Since, a certain limit $p\mathrm{CO_2}$ value in the free stream entails a higher $p\mathrm{CO_2}$ value in molecular contact with the organism surface, and effects for $p\mathrm{CO_2} = 5000\,\mu\mathrm{atm}$ are reported in Caldeira et al. (2005) for only the most sensitive organisms, choosing $p\mathrm{CO_2}|_\mathrm{s} = p\mathrm{CO_2}|_\mathrm{s}^\mathrm{max} = 5000\,\mu\mathrm{atm}$ is a rather low estimate for a limit value, likely overestimating the $\mathrm{CO_2}$ removal limitation in our calculations.

While we are aware that $p\mathrm{CO_2}|_\mathrm{s} = p\mathrm{CO_2}|_\mathrm{s}^\mathrm{max} = 5000\,\mu\mathrm{atm}$ is an assumption serving mainly exemplary purposes here, using one single constant value effectively also removes species dependency from the calculation of $\mathrm{RP_{CO_2}}$. The calculation may easily be repeated by substituting known species specific values. The sensitivity of our calculations with respect to $p\mathrm{CO_2}|_\mathrm{s}$ are explored below.

## 2.2 Maximal $\mathrm{CO_2}$ diffusion limited metabolic rate $E_\mathrm{max}^\mathrm{CO_2}$

Analogous to the oxygen quantity $E_\mathrm{max}$ (Hofmann et al., 2012), we can define a maximal metabolic rate ($\mathrm{CO_2}$ export and thus $\mathrm{O_2}$ import) that diffusive limitation of $\mathrm{CO_2}$ export would allow

$$E_\mathrm{max}^\mathrm{CO_2} := \frac{\mathrm{RP_{CO_2}}}{L^\mathrm{CO_2}} = \frac{D^\mathrm{CO_2}\,\rho_\mathrm{SW}\,K0'^\mathrm{CO_2}\,\mathrm{EF}}{L^\mathrm{CO_2}}\,\Delta p\mathrm{CO_2}|_\mathrm{DBL} \tag{16}$$

Title Page
Abstract | Introduction
Conclusions | References
Tables | Figures
◀| |▶
◀ ▶
Back | Close
Full Screen / Esc
Printer-friendly Version
Interactive Discussion

Here, we use the same generic description for $L^{\mathrm{CO_2}}$ (given in Table 1) as used for the EF definition (Eq. 9).

### 2.3 Required $\Delta p\mathrm{CO_2}|_{\mathrm{DBL}}$ for a given $E_{\mathrm{O2}}$

Similar to the $\mathrm{O_2}$ quantity $C_{\mathrm{f}}$ (Hofmann et al., 2012), we can define a quantity that is not dependent on the external $\mathrm{CO_2}$ content of the water. To explicitly include the dependence of gas exchange on partial pressure and the dependency of partial pressure on hydrostatic pressure (Enns et al., 1965), we assume a given oxygen uptake rate $E^{\mathrm{O_2}}$ (in µmol s$^1$ cm$^2$), experimentally determined at diffusivities and DBL thicknesses equal to the respective in-situ values, but at one atmosphere.

As stated in Eq. (1), we assume $E_{\mathrm{CO_2}} = E^{\mathrm{O_2}}$, with the flux directions defined as opposite. Therefore, we can calculate the required $\mathrm{CO_2}$ partial pressure differential (in µatm) that is able to support a given metabolic rate ($\mathrm{O_2}$ import and thus $\mathrm{CO_2}$ export) by making use of Eq. (13)

$$\Delta p\mathrm{CO_2}|_{\mathrm{DBL}} \geq \frac{E^{\mathrm{O_2}}\,L^{\mathrm{CO_2}}}{D^{\mathrm{CO_2}}\,\rho_{\mathrm{SW}}\,K0_{\mathrm{E—\,EF}}'^{\mathrm{CO_2}}} \tag{17}$$

where $K0_{\mathrm{E}}'^{\mathrm{CO_2}}$ is the apparent Henry's constant (calculated as eluded to above) at "experimental" conditions, i.e., at the conditions at which $E_{\mathrm{O_2}}$ was determined, most notably one atmosphere. Again, considering the limiting case of a minimal partial pressure differential that satisfies Eq. (17), we can define

$$\Delta p_{\mathrm{DBL}} := \frac{E^{\mathrm{O_2}}\,L^{\mathrm{CO_2}}}{D^{\mathrm{CO_2}}\,\rho_{\mathrm{SW}}\,K0_{\mathrm{E}}'^{\mathrm{CO_2}}\,\mathrm{EF}} \tag{18}$$

For exemplary purposes, we use $E^{\mathrm{O_2}} = 20 \times 10^{-7}$ µmol s$^{-1}$ cm$^{-2}$, consistent with the oxygen companion paper Hofmann et al. (2012).

### 2.4 Required minimal $pCO_2|_s$ for given external conditions and given $E^{O_2}$

Having calculated the minimally required $pCO_2$ gradient $\Delta p_{DBL}$ to sustain a given $E^{O_2}$ (and associated $E^{CO_2}$) from Eq. (18), a minimally required $pCO_2$ (in µatm) in molecular contact with the gas exchange surface of the organism can be calculated by using a given, pressure corrected (Enns et al., 1965) free stream (i.e., bulk ocean) $CO_2$ partial pressure $pCO_2|_f$

$$pCO_2|_s^{min} = pCO_2|_f + \Delta p_{DBL} \tag{19}$$

### 2.5 Maximal $pCO_2|_f$ for given $E^{O_2}$ and assumed $pCO_2|_s$

Similarly, the maximal external free stream $pCO_2$ permitting the efflux required for metabolic balance can be calculated. If the (maximal) $CO_2$ partial pressure $pCO_2|_s$ in contact with the respiratory surface that permits normal functioning of the animal is given, then

$$pCO_2|_f^{max} = pCO_2|_s - \Delta p_{DBL} \tag{20}$$

For illustrative purposes, we again assume $pCO_2|_s = pCO_2|_s^{max} = 5000\,\mu\text{atm}$ for calculations here.

### 2.6 Limiting external conditions for given $E^{O_2}$ and assumed $pCO_2|_s$

The quantity $pCO_2|_f^{max}$ can then be used to calculate the maximal, in situ, $CO_2$ concentration in the free stream bulk medium that is required for an experimentally observed $O_2$ demand to be supported as in

$$[CO_2]_f^{max} = pCO_2|_f^{max}\, K0'^{CO_2} \tag{21}$$

where $K0'^{CO_2}$ in mol kg$^{-1}$ atm$^{-1}$ is the apparent in-situ Henry's constant as calculated above (Eq. 4).

Title Page
Abstract | Introduction
Conclusions | References
Tables | Figures
◀| |▶
◀ ▶
Back | Close
Full Screen / Esc
Printer-friendly Version
Interactive Discussion

The property $[CO_2]_f^{max}$ can then be used to calculate limiting bulk fluid ocean conditions (e.g., maximal $[\sum CO_2]$: $[\sum CO_2]|_f^{max}$, minimal total scale pH: $pH|_f^{min}$, etc.) that can balance the required $O_2$ consumption. Bulk fluid free stream conditions here are calculated in the programming language R with the acid-base chemistry routines implemented in the R extension package AquaEnv (Hofmann et al., 2010), with the Millero et al. (2006) equilibrium constants for the carbonate system and all other constants being the standard AquaEnv formulations with references given there. $[\sum(BOH)_3]$, $[\sum H_2SO_4]$, and $[\sum HF]$ are estimated from salinity $S$ as given in DOE (1994) and Dickson et al. (2007). Conversions between free scale and total scale pH are done as implemented in AquaEnv.

## 2.7 External conditions: present-day and future values

In order to compare our derived example limiting free-stream conditions (maximal $p\mathrm{CO}_2$, $[\sum CO_2]$, and minimal pH) to present-day conditions we use data from the alkalinity and dissolved inorganic carbon climatology of Goyet et al. (2000) for a location off the coast of Southern California (SC: 120.5° W, 29.50° N) and other stations around the world (CH: Chile (75.5° W, 33.5° S); WP: Western Pacific (126.5° E, 11.5° N), WA: Western Africa (6.5° E, 15.5° S), MD: Mediterranean (18.5° E, 35.5° N); BB: Bay of Bengal (87.5° E, 18.5° N)), consistent with the oxygen companion paper Hofmann et al. (2012). Particularly, the southern California region is selected since it is well studied, and the eastern Pacific region shows strong vertical gradients in both $O_2$ and $CO_2$, thus ecompassing a wide range of oceanic values.

For future conditions we note that atmospheric $p\mathrm{CO}_2$ may approximately triple from pre-industrial by the end of the century (e.g., IPCC, 2007; Meehl et al., 2007) with well predicted oceanic $CO_2$ system consequences (e.g., Zeebe et al., 2008; Allison et al., 2009). We therefore assume a tripled $p\mathrm{CO}_2$ at all depths with associated increase in $[\sum CO_2]$ and decrease in pH, assuming constant alkalinity while recognizing that it will take several hundred years given the slow pace of oceanic mixing for changes of such scale to appear at depth.

## 3 Results and discussion

### 3.1 Sensitivity of $\mathrm{RP}_{\mathrm{CO}_2}$ and $E^{\mathrm{CO}_2}_{\max}$ with respect to $u_{100}$ and $p\mathrm{CO}_2|^{\max}_{\mathrm{s}}$

Figure 1 shows various plots that investigate the sensitivity of the two central derived quantities $\mathrm{RP}_{\mathrm{CO}_2}$ and $E^{\mathrm{CO}_2}_{\max}$ with respect to the input parameters $u_{100}$ and $p\mathrm{CO}_2|^{\max}_{\mathrm{s}}$. Both parameters are not accessible via typical oceanographic data and our calculations rely on assumed constant values for those parameters. Fig. 1 illustrates how our derived quantities depend on those input parameters and what the assumed values for them entail.

The left panel in the upper row of Fig. 1 shows that the EF dependency on $u_{100}$ is dominated by the dependency of the DBL thickness $L^{\mathrm{CO}_2}$ on $u_{100}$ (see Table 1 and the companion paper Hofmann et al. (2012) for details). Since $\mathrm{RP}_{\mathrm{CO}_2}$ depends linearly on EF (cf. Eq. 15), the EF dependency on $u_{100}$ exactly mirrors the $\mathrm{RP}_{\mathrm{CO}_2}$ dependency on $u_{100}$ (not shown).

EF increases with increasing temperature, rougly two-fold for a temperature increase from 1 °C to 25 °C (top left panel of Fig. 1). The general dependency of EF on $u_{100}$ is not affected by temperature.

The central panel in the top row of Fig. 1 shows that $\mathrm{RP}_{\mathrm{CO}_2}$ increases by about an order of magnitude in the $u_{100}$ range sampled, with the largest steps being exhibited for small $u_{100}$, which is consistent with the steep part of the curve of the EF dependency on $u_{100}$ for $u_{100}$ values below approximately $3\,\mathrm{cm\,s^{-1}}$.

The case of $\mathrm{EF} = 1$ completely eliminates the dependency of $\mathrm{RP}_{\mathrm{CO}_2}$ on $u_{100}$, but is equivalent to very large values of $u_{100}$. Consistently, the lowest values for $\mathrm{RP}_{\mathrm{CO}_2}$ are obtained with $\mathrm{EF} = 1$.

The right panel in the top row of Fig. 1 illustrates the linear dependency of $\mathrm{RP}_{\mathrm{CO}_2}$ on the $\mathrm{CO}_2$ partial pressure limit value in molecular contact with the organism $(p\mathrm{CO}_2|_s =)\, p\mathrm{CO}_2|_s^{\max}$. $\mathrm{RP}_{\mathrm{CO}_2}$ values increase from about $2 \times 10^{-6}\,\mu\mathrm{mol\,s}^{-1}$ to about $20 \times 10^{-6}\,\mu\mathrm{mol\,s}^{-1}$, when $p\mathrm{CO}_2|_s^{\max}$ increases from 2000 µatm to 20 000 µatm.

The better quantity to look at, however, when assessing the influence of the fluid flow velocity $u_{100}$ on the ability of the ocean to remove respiratory $\mathrm{CO}_2$ from the organism is the quantity $E_{\max}^{\mathrm{CO}_2}$. $\mathrm{RP}_{\mathrm{CO}_2}$ depends on EF which decreases with increasing $u_{100}$, i.e., in a thinner boundary layer, there is less time for the $\mathrm{CO}_2$ acid-base system to convert $\mathrm{CO}_2$ to carbonate and bicarbonate and thus effectively remove $\mathrm{CO}_2$ itself which enhances diffusion. However, $\mathrm{RP}_{\mathrm{CO}_2}$ does not incorporate the fact that with a thinner boundary layer, there is a shorter way for the $\mathrm{CO}_2$ to diffuse through, since the DBL thickness $L^{\mathrm{CO}_2}$ is removed from the definition to be consistent with the oxygen quantity $\mathrm{SP}_{O_2}$ in the companion paper. The quantity $E_{\max}^{\mathrm{CO}_2}$, however, does include this effect. The left panel in the bottom row of Fig. 1 shows that $E_{\max}^{\mathrm{CO}_2}$ increases steeply with increasing $u_{100}$, once $u_{100}$ has values above approximately $3\,\mathrm{cm\,s}^{-1}$. Below a free stream velocity of $3\,\mathrm{cm\,s}^{-1}$, $E_{\max}^{\mathrm{CO}_2}$ is virtually independent of $u_{100}$. For $u_{100}$ values larger than 5 $\mathrm{cm\ s}^{-1}$ the relation is almost linear. The overall positive correlation of $E_{\max}^{\mathrm{CO}_2}$ with $u_{100}$ shows that the effect of increasing flow decreasing the distance for diffusion ($L^{\mathrm{CO}_2}$ decreases with increasing $u_{100}$, which increases $E_{\max}^{\mathrm{CO}_2}$) dominates over the effect that this decreased distance allows for less time for the $\mathrm{CO}_2$ system to enhance the diffusive flux via chemical reactions (EF decreases with increasing $u_{100}$, which decreases $E_{\max}^{\mathrm{CO}_2}$).

$E_{\max}^{\mathrm{CO}_2}$ increases with increasing temperature, also about two-fold for a temperature increase from 1 °C to 25 °C (bottom left panel of Fig. 1). It can be seen that the dependency of $E_{\max}^{\mathrm{CO}_2}$ on $u_{100}$ is less pronounced for higher temperatures.

Comparing the central panels in upper and bottom rows of Fig. 1 illustrates the difference in DBL thicknes $L^{\mathrm{CO_2}}$ (i.e., $u_{100}$) dependency of $\mathrm{RP_{CO_2}}$ and $E_{\mathrm{max}}^{\mathrm{CO_2}}$. While $\mathrm{RP_{CO_2}}$ shows a strong negative correlation with $u_{100}$ (central panel, top row Fig. 1), $E_{\mathrm{max}}^{\mathrm{CO_2}}$, exhibits a moderate positive correlataion with $u_{100}$. As already mentioned above, the effect of less distance for diffusion with increasing $u_{100}$ outweighs the effect of less time for chemical enhancement of the flux with increasing $u_{100}$. However, due to the combination of those two counteracting effects, the net dependency of $E_{\mathrm{max}}^{\mathrm{CO_2}}$ on $u_{100}$ is much less pronounced than the dependency of $\mathrm{RP_{CO_2}}$ on $u_{100}$ and also the dependency of $\mathrm{SP_{O_2}}$ (Hofmann et al., 2012) on $u_{100}$. In the central panel of the bottom row of Fig. 1, it can also clearly be seen that the dependency of $E_{\mathrm{max}}^{\mathrm{CO_2}}$ on $u_{100}$ is less pronounced at shallower depths with higher temperatures and pH values than at deeper depths with colder temperatures and lower pH values.

In the case of $\mathrm{EF} = 1$, one assumes an effect of $u_{100}$ on $L^{\mathrm{CO_2}}$, i.e., decreasing the distance for diffusion with increasing flow velocity, but the effect of chemical enhancement in a thick DBL is neglected. Therefore, the $\mathrm{EF} = 1$ case here shows the lowest values for $E_{\mathrm{max}}^{\mathrm{CO_2}}$ although for the calculation of $L^{\mathrm{CO_2}}$ an intermediate value of $6\,\mathrm{cm\,s^{-1}}$ is used for $u_{100}$.

The right panel in the bottom row of Fig. 1 shows that the dependency on $p\mathrm{CO_2}|_{\mathrm{s}}^{\mathrm{max}}$ is similar for $E_{\mathrm{max}}^{\mathrm{CO_2}}$ and $\mathrm{RP_{CO_2}}$.

## 3.2 Example depth profiles for various stations around the world

Figure 2 shows $\mathrm{RP_{CO_2}}$ depth profiles for example stations around the world (top panels) It can be clearly seen, that the profiles are overall dominated by the enhancement factor (bottom panels), which exhibits rather similar values for deeper depths between all profiles, but differs for depths shallower then 500 m due to different temperature and pH profiles (due to its dependency on $[\mathrm{OH^-}]$, EF depends positively on pH, see Eq. 9 to 11.) This dependency of EF on pH is also the reason for the fact that the profile for the

Mediterranean (MD) shows markedly higher EF and thus $RP_{CO_2}$ values than profiles for the other stations, as the mediterranean profile exhibits higher alkalinity (central panels of Fig. 3) and thus lower $p\mathrm{CO}_2$ (bottom panels of Fig. 3) and higher pH (not shown).

The specific shapes of and the differences between $RP_{CO_2}$ profiles, especially at deeper depths, is caused by differing $p\mathrm{CO}_2$ profiles, as the central panels of Fig. 4 ($RP_{CO_2}$, with EF = 1) show when compared to $p\mathrm{CO}_2$ profiles of the respective stations (bottom panels of Fig. 3). Off the coast of Chile (station CH), a clear $p\mathrm{CO}_2$ maximum can be identified shallower than 500 m (bottom left panel of Fig. 3), which results in a local dip in $RP_{CO_2}$ values (top left panel of Fig. 2), and which is due to a local $[\sum \mathrm{CO}_2]$ maximum (top left panel of of Fig. 3). This region corresponds to the local oxygen minimum in this region as described in the companion paper Hofmann et al. (2012).

Figure 4 shows $E_{\mathrm{max}}^{\mathrm{CO}_2}$ depth profiles. As expected, the general shape of the profiles is the same as for $RP_{CO_2}$, as $E_{\mathrm{max}}^{\mathrm{CO}_2}$ is calculated by dividing $RP_{CO_2}$ by $L^{\mathrm{CO}_2}$ which is calculated using a constant $u_{100}$ of 6 cm s$^{-1}$.

The top panels of Fig. 5 show depth profiles of $\Delta p_{\mathrm{DBL}}$, the $\mathrm{CO}_2$ partial pressure differential across the DBL that is required to sustain a given oxygen uptake and resulting $\mathrm{CO}_2$ export. It can clearly be seen, that $\Delta p_{\mathrm{DBL}}$ decreases with depth and decreasing temperature. The $\Delta p_{\mathrm{DBL}}$ profiles are rather similar for all stations, with a pronounced difference for the Mediterranean (MD) station, most likely due to high temperatures and [TA] values (see also Fig. 3).

In the bottom panels of Fig. 5 depth profiles of $p\mathrm{CO}_2|_s^{\mathrm{min}}$, the minimal $\mathrm{CO}_2$ partial pressure in molecular contact with the organism surface that is required to drive a given metabolic flux across the DBL, are given. The general shape of the profiles are dominated by ambient $p\mathrm{CO}_2$ profiles (Fig. 3), but for all stations except the Mediterranean station (MD), values at depth are considerably higher for $p\mathrm{CO}_2|_s^{\mathrm{min}}$ than for ambient $p\mathrm{CO}_2$ due to the higher $\Delta p_{\mathrm{DBL}}$ values caused by lower temperatures.

### 3.3 Diffusive CO$_2$ limitation? Present and future conditions

Having calculated a $pCO_2|_f^{max}$ (the maximal $p$CO$_2$ in the free stream that can support a given metabolic rate) profile for the Southern California (SC) station, we calculated limiting external conditions from that: the maximal external dissolved inorganic carbon concentration $[\sum \mathrm{CO_2}]_\mathrm{f}^\mathrm{max}$, and the minimal free stream, total scale pH $\mathrm{pH}|_\mathrm{f}^\mathrm{min}$. Figure 6 shows profiles of those external limit conditions (black lines) and compares them to present-day ambient conditions extracted from the Goyet et al. (2000) climatology (blue lines). It can be seen that present-day ambient conditions are rather far away from the calculated limit conditions. However, crudely assumed future conditions (i.e., a tripling of $p$CO$_2$ in the whole water column by appropriate theoretical addition of dissolved inorganic carbon), show that there is a region at about 700 m depth at this station, where diffusive CO$_2$ export could become close to limiting, given the assumed metabolic rate of $E^{\mathrm{O_2}} = 20 \times 10^{-7}$ µmol s$^{-1}$ cm$^{-2}$.

### 3.4 Diffusive CO$_2$ limitation vs. diffusive O$_2$ limitation

Figure 7 compares depth profiles for the Southern California station (SC) of the equivalent diffusive oxygen and carbon dioxide limitation quantities $\mathrm{SP}_{O_2}$ and $\mathrm{RP}_{\mathrm{CO_2}}$, as well as $E^{\mathrm{O_2}}_{\mathrm{max}}$ (called $E_{\mathrm{max}}$ in Hofmann et al., 2012) and $E^{\mathrm{CO_2}}_{\mathrm{max}}$.

The left panel of Fig. 7 compares $\mathrm{SP}_{\mathrm{O_2}}$ (red line) and $\mathrm{RP}_{\mathrm{CO_2}}$, calculated with a fluid flow velocity of 2 cm s$^{-1}$ (black line). $\mathrm{SP}_{vO_2}$ values are considerably lower than $\mathrm{RP}_{\mathrm{CO_2}}$ values throughout the whole water column, suggesting that diffusive limitation of oxygen uptake is dominant over diffusive limitation of respiratory carbon dioxide export. Comparing present-day $\mathrm{SP}_{\mathrm{O_2}}$ values with $\mathrm{RP}_{\mathrm{CO_2}}$ calculated with assumed future conditions (i.e., a tripled $p$CO$_2$ throughout the whole water column, blue line), still reveals a dominance of diffusive oxygen limitation over diffusive carbon dioxide export limitation. And this is without assuming any decline in oceanic oxygenation, which would decrease $\mathrm{SP}_{\mathrm{O_2}}$ values even further and would thus amplify the dominance of oxygen limitaion over carbon dioxide limitation. It must be noted, however, that, although both quantities are defined as equivalent as possible, $\mathrm{RP}_{\mathrm{CO}_2}$ still depends on the free stream water velocity $u_{100}$ via the enhancement factor EF. $\mathrm{RP}_{\mathrm{CO}_2}$ values here are calculated with the rather low velocity of $2\,\mathrm{cm\,s^{-1}}$, to assume a rather high diffusive $CO_2$ limitation, yet, $\mathrm{SP}_{\mathrm{O}_2}$ and $\mathrm{RP}_{\mathrm{CO}_2}$ are not optimal quantities when comparing diffusive oxygen uptake limitation to diffusive carbon dioxide export limitation.

The better quantity-pair to this end is the pair $E_{\mathrm{max}}^{\mathrm{O}_2}$ and $E_{\mathrm{max}}^{\mathrm{CO}_2}$, as both quantities similarly depend on the free stream water velocity, and if the same DBL model description is used for both quantities, a relative comparison between both quantities will be valid and meaningful. The right panel of Fig. 7 compares $E_{\mathrm{max}}^{\mathrm{O}_2}$ and $E_{\mathrm{max}}^{\mathrm{CO}_2}$ values calculated with different free stream water velocities $u_{100}$. Even comparing $E_{\mathrm{max}}^{\mathrm{O}_2}$ values calculated with $u_{100} = 6\,\mathrm{cm\,s^{-1}}$ (orange line), to $E_{\mathrm{max}}^{\mathrm{CO}_2}$ values calculated with $u_{100} = 2\,\mathrm{cm\,s^{-1}}$, which artificially favors $CO_2$ limitation, confirms the dominance of diffusive oxygen uptake limitation over diffusive carbon dioxide export limitation. Only $E_{\mathrm{max}}^{\mathrm{CO}_2}$ values calculated with a future tripled $p\mathrm{CO}_2$ and $2\,\mathrm{cm\,s^{-1}}$ (red line) are close to $E_{\mathrm{max}}^{\mathrm{O}_2}$ values calculated with $6\,\mathrm{cm\,s^{-1}}$ (orange line), which is an artificial case, strongly favoring $CO_2$ limitation.

Important to note is that the value for $p\mathrm{CO}_2|_\mathrm{s}$ used here is deliberately chosen to be comparatively low, i.e., only the most sensitive organisms show reactions in Caldeira et al. (2005), so that the defined $CO_2$ limiting quantities likely overestimate the $CO_2$ removal limitation. So when compared to the equivalent oxygen supply limitation quantities, highest conceivable $CO_2$ export limitations are considered. Still, diffusive oxygen uptake limitation seems to be dominant, due to the chemical enhancement of the diffusive $CO_2$ export.

## 4 Conclusions and outlook

The ocean is now undergoing simultaneous warming, loss of $O_2$, and rising $CO_2$ levels. The impact of changes in each of these properties draws intense scientific scrutiny but ways in which the ensemble effect can be estimated are few. In a first attempt to address the combined impacts Brewer and Peltzer (2009) defined a "respiration index" which linked the ratios of $pO_2$ to $pCO_2$ via the simple form of the Gibbs' free energy equation. This paper, by converting traditional properties such as a simple mass values for $[O_2]$ into the partial pressures that can accommodate changing temperature and correctly represent the driving force for respiration, is an attempt to assess the relative hospitability of certain ocean regions to support aerobic respiration (e.g., Mayol et al., 2012).

Our findings here, and in the oxygen companion paper, that it is energetically easier to transport $CO_2$ away from an organism due to the chemical enhancement term than to bring $O_2$ towards it which requires physical changes in diffusive boundary layer thickness, suggests a route towards an improved function. In this function, estimating only physical processes originating in the external ocean, declines in $pO_2$ would be given more weight than increases in $pCO_2$.

Although neither impact is positive for marine life, considering only diffusive limitation effects, global warming/declining $O_2$ is most likely a greater threat to most oceanic life than is oceanic uptake of antropogenic $CO_2$. However, there might be further respiratory effects of $CO_2$ input and acidification that are not considered here: such as oxygen transport mechanisms in animals are impacted by an elevated proton concentration (e.g., Seibel and Walsh, 2003) and the decrease of the free energy yield of the respiration reaction (Brewer and Peltzer, 2009).

Of course, as already widely studied and well known, ocean acidification due to anthropogenic $CO_2$ uptake of the oceans results in a decrease in the carbonate ion concentration with negative effects on biogenic calcification. Animals will have to expend energy in an effort to reduce the loss of carbonate shell protection. This means

$O_2$ dependent processes will have to be increased, in principle favoring non-calcifying organisms in high $CO_2$ low $O_2$ regions, and thus establishing a more direct linkage between $O_2$ and $CO_2$ in the ocean.

*Acknowledgements.* This work was supported by a grant to the Monterey Bay Aquarium Research Institute from the David & Lucile Packard Foundation.

## References

Allen, M. R., Frame, D. J., Huntingford, C., Jones, C. D., Lowe, J. A., Meinshausen, M., and Meinshausen, N.: Warming caused by cumulative carbon emissions towards the trillionth tonne, Nature, 458, 1163–1166, doi:10.1038/nature08019, 2009. 15790

Allison, I., Bindoff, N. L., Bindschadler, R. A., Cox, P. M., de Noblet, N., England, M. H., Francis, J. E., Gruber, N., Haywood, A. M., Karoly, D. J., Kaser, G., Le Quéré, C., Lenton, T. M., Mann, M. E., McNeil, B. I., Pitman, A. J., Rahmstorf, S., Rignot, E., Schellnhuber, H. J., Schneider, S. H., Sherwood, S. C., Somerville, R. C. J., Steffen, K., Steig, E. J., Visbeck, M., and Weaver, A.: The Copenhagen Diagnosis: Updating the world on the Latest Climate Science, The University of New South Wales Climate Change Research Centre (CCRC), Sydney, Australia, 60 pp., 2009. 15790, 15800

Archer, D.: Modeling $CO_2$ in the Ocean: a review, in: Scaling of Trace Gas Fluxes between Terrestrial and Aquatic Ecosystems and the Atmosphere, edited by: Bouwman, A. F., 24, 169–184, Elsevier Sciences, Amsterdam, 1999. 15790

Archer, D.: Fate of fossil fuel $CO_2$ in geologic time, J. Geophys. Res.-Oceans, 110, C09S05, doi:10.1029/2004JC002625, 2005. 15790

Archer, D., Kheshgi, H., and Maier-Reimer, E.: Dynamics of fossil fuel $CO_2$ neutralization by marine $CaCO_3$, Global Biogeochem. Cy., 12, 259–276, 1998. 15790

Archer, D., Eby, M., Brovkin, V., Ridgwell, A., Cao, L., Mikolajewicz, U., Caldeira, K., Matsumoto, K., Munhoven, G., Montenegro, A., and Tokos, K.: Atmospheric Lifetime of Fossil Fuel Carbon Dioxide, Annu. Rev. Earth Pl. Sc., 37, 117–134, doi:10.1146/annurev.earth.031208.100206, 2009. 15790

Biron, P. M., Robson, C., Lapointe, M. F., and Gaskin, S. J.: Comparing different methods of bed shear stress estimates in simple and complex flow fields, Earth Surf. Proc. Land., 29, 1403–1415, doi:10.1002/esp.1111, 2004. 15814

Blackford, J. C. and Gilbert, F. J.: pH variability and $CO_2$ induced acidification in the North Sea, J. Mar. Syst., 64, 229–241, 2007. 15789

Boudreau, B. P.: A method-of-lines code for carbon and nutrient diagenesis in aquatic sediments, Comput. Geosci., 22, 479–496, 1996. 15814

Brewer, P. and Peltzer, E.: Limits to Marine Life, Science, 324, 347–348, 2009. 15807

Brewer, P. G., Friederich, G., Peltzer, E. T., and Orr Jr., F. M.: Direct Experiments on the Ocean Disposal of Fossil Fuel $CO_2$, Science, 284, 943–945, doi:10.1126/science.284.5416.943, 1999. 15789

Bryden, H. L.: New polynomials for thermal expansion, adiabatic temperature gradient and potential temperature of sea water, Deep-Sea Res., 20, 401–408, 1973. 15792

Caldeira, K. and Wickett, M. E.: Anthropogenic carbon and ocean pH, Nature, 425, 365–365, 2003. 15789

Caldeira, K. and Wickett, M. E.: Ocean model predictions of chemistry changes from carbon dioxide emissions to the atmosphere and ocean, J. Geophys. Res.-Oceans, 110, C09S04, doi:10.1029/2004JC002671, 2005. 15789

Caldeira, K., Akai, M., Brewer, P., Chen, B., Haugan, P., Iwama, T., Johnston, P., Kheshgi, H., Li, Q., Ohsumi, T., Pörtner, H. O., Sabine, C., Shirayama, Y., Thomson, J., Barry, J., and Hansen, L.: Ocean Storage, in: IPCC Special Report on Carbon dioxide Capture and Storage, IPCC, 2005. 15789, 15790, 15797, 15806

Dickson, A. G., Sabine, C., and Christian, J. R.: Guide to best practices for ocean $CO_2$ measurements, PICES Special Publications, 1–191, 2007. 15800

DOE: Handbook of Methods for the Analysis of the Various Parameters of the Carbon Dioxide System in Sea Water, ORNL/CDIAC-74, 1994. 15800

Emerson, S.: Chemically Enhanced Carbon Di Oxide Gas Exchange In A Eutrophic Lake A General Model, Limnol. Oceanogr., 20, 743–761, 1975. 15793

Enns, T., Scholander, P. F., and Bradstreet, E. D.: Effect of Hydrostatic Pressure on Gases Dissolved in Water, J. Phys. Chem., 69, 389–391, 1965. 15792, 15798, 15799

Fofonoff, N. P.: Computation of potential temperature of seawater for an arbitrary reference pressure, Deep-Sea Res., 24, 489–491, 1977. 15792

Fofonoff, N. P. and Millard, R. C. J.: Algorithms for computation of fundamental properties of seawater, UNESCO Technical Papers in Marine Science, 44, 55 pp., 1983. 15792

Garcia, H. E., Locarnini, R. A., Boyer, T. P., Antonov, J. I., Baranova, O. K., Zweng, M. M., and Johnson, D. R.: World Ocean Atlas 2009, Volume 3: Dissolved Oxygen, Apparent Oxygen Utilization, and Oxygen Saturation., NOAA Atlas NESDIS 70, edited by: Levitus, S., US Government Printing Office, Washington, DC, 344 pp., 2010. 15821

Gattuso, J. P., Frankignoulle, M., Bourge, I., Romaine, S., and Buddemeier, R. W.: Effect of calcium carbonate saturation of seawater on coral calcification, Global Planet. Change, 18, 37–46, doi:10.1016/S0921-8181(98)00035-6, 1998. 15789

Goyet, C., Healy, R. J., and Ryan, J. P.: Global distribution of total inorganic carbon and total alkalinity below the deepest winter mixed layer depths, ORNL/CDIAC-127, NDP-076, Carbon Dioxide Information Analysis Center, Oak Ridge National Laboratory, US Department of Energy, Oak Ridge, Tennessee, 40 pp., 2000. 15800, 15805, 15815, 15816, 15817, 15818, 15819, 15820, 15821

Haugan, P. M.: On the production and use of scientific knowledge about ocean sequestration, in: Greenhouse Gas Control Technologies, edited by: Gale, J. and Kaya, Y., 1, 719–724, Proceedings of the 6th International Conference on Greenhouse Gas Control Technolgies, Elsevier, 2003. 15789

Hickey, B., Baker, E., and Kachel, N.: Suspended particle movement in and around Quinault submarine canyon, Mar. Geol., 71, 35–83, doi:10.1016/0025-3227(86)90032-0, 1986. 15814

Hofmann, A. F., Meysman, F. J. R., Soetaert, K., and Middelburg, J. J.: A step-by-step procedure for pH model construction in aquatic systems, Biogeosciences, 5, 227–251, doi:10.5194/bg-5-227-2008, 2008. 15793

Hofmann, A. F., Soetaert, K., Middelburg, J. J., and Meysman, F. J. R.: AquaEnv : An Aquatic Acid-Base Modelling Environment in R, Aquat. Geochem., 16, 507–546, 2010. 15792, 15793, 15794, 15800

Hofmann, A. F., Peltzer, E. T., and Brewer, P. G.: Kinetic bottlenecks to chemical exchange rates for deep-sea animals – Part 1: Oxygen, Biogeosciences Discuss., 9, 13817–13856, doi:10.5194/bgd-9-13817-2012, 2012. 15789, 15791, 15792, 15795, 15796, 15797, 15798, 15800, 15801, 15803, 15804, 15805, 15821

IPCC: Climate Change 2007: Synthesis Report, Contributions of Working Groups I, II, and III to the Fourth Assessment Report of the Intergovernmental Panel on Climate Change, Tech. rep., Geneva, Switzerland, 2007. 15789, 15790, 15800

Kita, J. and Ohsumi, T.: Perspectives on Biological Research for $CO_2$ Ocean Sequestration, J. Oceanogr., 60, 695–703, doi:10.1007/s10872-004-5762-1, 2004. 15789

Koertzinger, A.: Determination of carbon dioxide partial pressure ($p$CO$_2$), in: Methods of Seawater Analysis, edited by: Grasshoff, K., Kremling, K., and Erhardt, M., 149–158, Wiley-VCH, Weinheim, 1999. 15792

Marchetti, C.: On geoengineering and the CO$_2$ problem, Climatic Change, 1, 59–68, doi:10.1007/BF00162777, 1977. 15789

Mayol, E., Ruiz-Halpern, S., Duarte, C. M., Castilla, J. C., and Pelegrí, J. L.: Coupled CO$_2$ and O$_2$-driven compromises to marine life in summer along the Chilean sector of the Humboldt Current System, Biogeosciences, 9, 1183–1194, doi:10.5194/bg-9-1183-2012, 2012. 15807

Meehl, G. A., Stocker, T. F., Collins, W. D., Friedlingstein, P., Gaye, A. T., Gregory, J. M., Kitoh, A., Knutti, R., Murphy, J. M., Noda, A., Raper, S. C. B., Watterson, I. G., Weaver, A. J., and Zhao, Z.-C.: Global Climate Projections, in: Climate Change 2007: The Physical Science Basis. Contribution of Working Group I to the Fourth Assessment Report of the Intergovernmental Panel on Climate Change, edited by: Solomon, S., Qin, D., Manning, M., Chen, Z., Marquis, M., Averyt, K. B., Tignor, M., and Miller, H. L., Cambridge University Press, Cambridge, UK and New York, NY, USA, 2007. 15789, 15800

Millero, F. J.: Thermodynamics of the Carbon-Dioxide System in the Oceans, Geochim. Cosmochim. Ac., 59, 661–677, 1995. 15794

Millero, F. J. and Poisson, A.: International One-Atmosphere Equation of State of Seawater, Deep-Sea Res., 28, 625–629, 1981. 15792

Millero, F. J., Graham, T. B., Huang, F., Bustos-Serrano, H., and Pierrot, D.: Dissociation constants of carbonic acid in seawater as a function of salinity and temperature, Mar. Chem., 100, 80–94, 2006. 15800

Orr, J. C., Fabry, V. J., Aumont, O., Bopp, L., Doney, S. C., Feely, R. A., Gnanadesikan, A., Gruber, N., Ishida, A., Joos, F., Key, R. M., Lindsay, K., Maier-Reimer, E., Matear, R., Monfray, P., Mouchet, A., Najjar, R. G., Plattner, G. K., Rodgers, K. B., Sabine, C. L., Sarmiento, J. L., Schlitzer, R., Slater, R. D., Totterdell, I. J., Weirig, M. F., Yamanaka, Y., and Yool, A.: Anthropogenic ocean acidification over the twenty-first century and its impact on calcifying organisms, Nature, 437, 681–686, 2005. 15789

Perry, S. F., Braun, M. H., Genz, J., Vulesevic, B., Taylor, J., Grosell, M., and Gilmour, K. M.: Acid-base regulation in the plainfin midshipman (Porichthys notatus): an aglomerular marine teleost, J. Comp. Physiol. B, 180, 1213–1225, 2010. 15790

Pinczewski, W. V. and Sideman, S.: A model for mass (heat) transfer in turbulent tube flow, Moderate and high Schmidt (Prandtl) numbers, Chem. Eng. Sci., 29, 1969–1976, doi:10.1016/0009-2509(74)85016-5, 1974. 15814

Poertner, H. O., Langenbuch, M., and Michaelidis, B.: Synergistic effects of temperature extremes, hypoxia, and increases in $CO_2$ on marine animals: From Earth history to global change, J. Geophys. Res.-Oceans, 110, C09S10, doi:10.1029/2004JC002561, 2005. 15797

Royal Society: Ocean Acidification Due to Increasing Atmospheric Carbon Doxide, Policy Document 12/05, The Royal Society, London, UK, 2005. 15789

Sabine, C. L., Feely, R. A., Gruber, N., Key, R. M., Lee, K., Bullister, J. L., Wanninkhof, R., Wong, C. S., Wallace, D. W. R., Tilbrook, B., Millero, F. J., Peng, T. H., Kozyr, A., Ono, T., and Rios, A. F.: The oceanic sink for anthropogenic $CO_2$, Science, 305, 367–371, 2004. 15790

Santschi, P. H., Anderson, R. F., Fleisher, M. Q., and Bowles, W.: Measurements of Diffusive Sublayer Thicknesses in the Ocean by Alabaster Dissolution, and Their Implications for the Measurements of Benthic Fluxes, J. Geophys. Res., 96, 10641–10657, 1991. 15814

Sarmiento, J. L. and Toggweiler, J. R.: A New Model for the Role of the Oceans in Determining Atmospheric $PCO_2$, Nature, 308, 621–624, 1984. 15790

Sarmiento, J. L., Le Quéré, C., and Pacala, S. W.: Limiting future atmospheric carbon dioxide, Global Biogeochem. Cy., 9, 121–137, doi:10.1029/94GB01779, 1995. 15790

Seibel, B. A. and Walsh, P. J.: Potential Impacts of $CO_2$ Injection on Deep-Sea Biota, Science, 294, 319–320, doi:10.1126/science.1065301, 2001. 15790

Seibel, B. A. and Walsh, P. J.: Biological impacts of deep-sea carbon dioxide injection inferred from indices of physiological performance, J. Exp. Biol., 206, 641–650, 2003. 15790, 15807

Shaffer, G., Olsen, S. M., and Pedersen, J. O. P.: Long-term ocean oxygen depletion in response to carbon dioxide emissions from fossil fuels, Nat. Geosc., 2, 105–109, doi:10.1038/NGEO420, 2009. 15789, 15790

Shaw, D. A. and Hanratty, T. J.: Turbulent mass transfer rates to a wall for large Schmidt numbers, AICHE J., 23, 28–37, doi:10.1002/aic.690230106, 1977. 15814

Siegenthaler, U. and Wenk, T.: Rapid Atmospheric $CO_2$ Variations and Ocean Circulation, Nature, 308, 624–626, 1984. 15790

Soetaert, K., Petzoldt, T., and Meysman, F.: marelac: Tools for Aquatic Sciences, available at: http://CRAN.R-project.org/package=marelac, r package version 2.1, 2010. 15814

Sternberg, R. W.: Friction factors in tidal channels with differing bed roughness, Mar. Geol., 6, 243–260, doi:10.1016/0025-3227(68)90033-9, 1968. 15814

Wanninkhof, R.: Relationship between Wind-Speed and Gas-Exchange over the Ocean, J. Geophys. Res.-Oceans, 97, 7373–7382, 1992. 15814

Weiss, R. F.: Carbon dioxide in water and seawater: the solubility of a non-ideal gas, Mar. Chem., 2, 203–215, 1974. 15792

Wood, P. E. and Petty, C. A.: New model for turbulent mass transfer near a rigid interface, AICHE J., 29, 164–167, doi:10.1002/aic.690290126, 1983. 15814

Zeebe, R. E. and Wolf-Gladrow, D.: $CO_2$ in Seawater: Equilibrium, Kinetics, Isotopes, no. 65 in: Elsevier Oceanography Series, Elsevier, first edn., 2001. 15792, 15793, 15794, 15795

Zeebe, R. E., Zachos, J. C., Caldeira, K., and Tyrrell, T.: Oceans – Carbon emissions and acidification, Science, 321, 51–52, 2008. 15789, 15800

**Table 1.** Expressing the DBL thickness $L$ as a function of water flow velocity: a generic planar surface description.

---

The DBL thickness for $CO_2$ $L^{CO_2}$ can be expressed as the fraction of the temperature-dependent molecular diffusion coefficient $D^{CO_2}$ for $CO_2$ in $cm^2\,s^{-1}$, calculated from temperature and salinity as given in Boudreau (1996, Chapter 4) using the implementation in the R package marelac (Soetaert et al., 2010), and the mass transfer coefficient $K_{CO_2}$ (Santschi et al., 1991; Boudreau, 1996)

$$L^{CO_2} = \frac{D^{CO_2}}{K_{CO_2}} \tag{22}$$

$K_{CO_2}$ can be calculated for $CO_2$ from the water-flow induced shear velocity $u'$ in $cm\,s^{-1}$ and the dimensionless Schmidt number $Sc$ for $CO_2$ (as calculated by linearly interpolating two temperature dependent formulations for $S = 35$ and $S = 0$ in Wanninkhof (1992) with respect to given salinity)

$$K_{CO_2} = a\, u'\, Sc_{CO_2}^{-b} \tag{23}$$

with parameters $a$ and $b$: Santschi et al. (1991): $a = 0.078$, $b = \frac{2}{3}$; Shaw and Hanratty (1977) (also given in Boudreau, 1996): $a = 0.0889$, $b = 0.704$; Pinczewski and Sideman (1974) as given in Boudreau (1996): $a = 0.0671$, $b = \frac{2}{3}$; Wood and Petty (1983) as given in Boudreau (1996): $a = 0.0967$, $b = \frac{7}{10}$. Due to small differences we use averaged results of all formulations.

$u'$ can be calculated from the ambient current velocity at 100 cm away from the exchange surface $u_{100}$ and the dimensionless drag coefficient $c_{100}$ (Sternberg, 1968; Santschi et al., 1991; Biron et al., 2004)

$$u' = u_{100}\,\sqrt{c_{100}} \tag{24}$$

$c_{100}$ is calculated from the water flow velocity $u_{100}$ as (Hickey et al., 1986; Santschi et al., 1991)

$$c_{100} = 10^{-3}\,\left(2.33 - 0.0526\,|u_{100}| + 0.000365\,|u_{100}|^2\right) \tag{25}$$

Title Page
Abstract Introduction
Conclusions References
Tables Figures
◂◂ ▸▸
◂ ▸
Back Close
Full Screen / Esc
Printer-friendly Version
Interactive Discussion

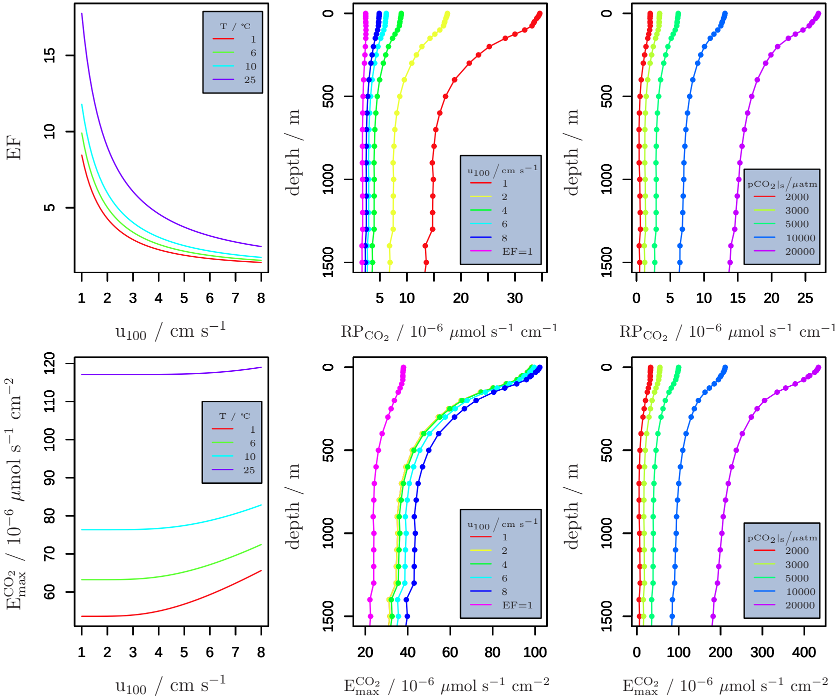

**Fig. 1.** Sensitivity of derived quantities RP$_{\mathrm{CO_2}}$ (the oceanic CO$_2$ removal potential) and $E_{\mathrm{max}}^{\mathrm{CO_2}}$ (the maximal CO$_2$ diffusion limited metabolic rate) with respect to the free stream fluid flow velocity $u_{100}$ and the maximal CO$_2$ partial pressure in molecular contact with the organism surface (($p\mathrm{CO_2}|_\mathrm{s}$ =) $p\mathrm{CO_2}|_\mathrm{s}^{\mathrm{max}}$). Left panel, upper row: the enhancement factor EF as a function of the free stream fluid flow velocity $u_{100}$ and temperature $T$. $[\sum\mathrm{CO_2}] = 1900\,\mu\mathrm{mol\,kg^{-1}}$, $[\mathrm{TA}] = 2050\,\mu\mathrm{mol\,kg^{-1}}$, $S = 34$, detph = 100 m, latitude = 30°. Central panel, upper row: example depth profiles at the Southern California (SC: 120.5° W, 29.50° N) station (data from Goyet et al., 2000) of RP$_{\mathrm{CO_2}}$, calculated with varying free stream fluid flow velocities $u_{100}$ and assuming EF = 1. $p\mathrm{CO_2}|_\mathrm{s}^{\mathrm{max}} = 5000\,\mu\mathrm{atm}$. Right panel, upper row: example depth profiles at the Southern California (SC) station of RP$_{\mathrm{CO_2}}$, calculated with varying values for the CO$_2$ partial pressure in molecular contact with the organism surface ($p\mathrm{CO_2}|_\mathrm{s}$ =) $p\mathrm{CO_2}|_\mathrm{s}^{\mathrm{max}}$. $u_{100} = 6\,\mathrm{cm\,s^{-1}}$. Left panel, bottom row: $E_{\mathrm{max}}^{\mathrm{CO_2}}$ as a function of the free stream fluid flow velocity $u_{100}$ and temperature $T$. $[\sum\mathrm{CO_2}] = 1900\,\mu\mathrm{mol\,kg^{-1}}$, $[\mathrm{TA}] = 2050\,\mu\mathrm{mol\,kg^{-1}}$, $S = 34$, detph = 100 m, latitude = 30 °, $p\mathrm{CO_2}|_\mathrm{s}^{\mathrm{max}} = 5000\,\mu\mathrm{atm}$. Central panel, bottom row: example depth profiles at the Southern California (SC) station of $E_{\mathrm{max}}^{\mathrm{CO_2}}$, calculated with varying free stream fluid flow velocities $u_{100}$ and assuming EF = 1. $p\mathrm{CO_2}|_\mathrm{s}^{\mathrm{max}} = 5000\,\mu\mathrm{atm}$. $u_{100} = 6\,\mathrm{cm\,s^{-1}}$ for the calculation of $L^{\mathrm{CO_2}}$ in the EF = 1 case. Right panel, bottom row: Example depth profiles at the Southern California (SC) station of $E_{\mathrm{max}}^{\mathrm{CO_2}}$, calculated with varying values for the CO$_2$ partial pressure in molecular contact with the organism surface ($p\mathrm{CO_2}|_\mathrm{s}$ =) $p\mathrm{CO_2}|_\mathrm{s}^{\mathrm{max}}$. $u_{100} = 6\,\mathrm{cm\,s^{-1}}$.

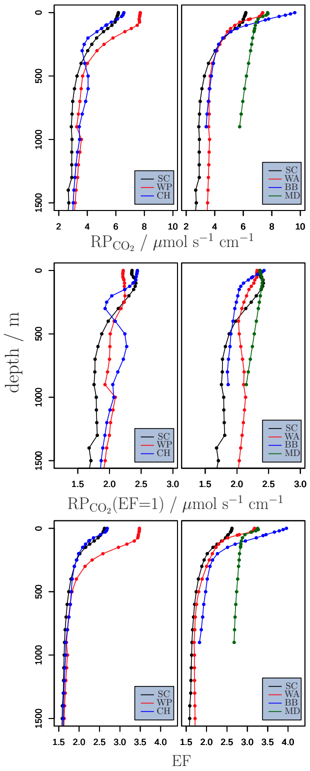

**Fig. 2.** Example depth profiles of the derived diffusive $CO_2$ export limitation quantity $RP_{CO_2}$ (the oceanic $CO_2$ removal potential). Top row: $RP_{CO_2}$ calculated using the chemical enhancement factor EF according to Eq. (9) with $u_{100} = 6$ cm s$^{-}$1. Central row: $RP_{CO_2}$ calculated assuming no chemical enhancement (i.e., EF = 1). Bottom row: EF calculated according to Eq. (9) with $u_{100} = 6$ cm s$^{-}$1. $pCO_2|_s^{max} = 5000$ µatm. Oceanographical data are taken from Goyet et al. (2000) and limited to shallower depths when discontinuities occurred deeper (SC: Southern California (120.5° W, 29.50° N); CH: Chile (75.5° W, 33.5° S); WP: Western Pacific (126.5° E, 11.5° N), WA: Western Africa (6.5° E, 15.5° S), MD: Mediterranean (18.5° E, 35.5° N); BB: Bay of Bengal (87.5° E, 18.5° N)).

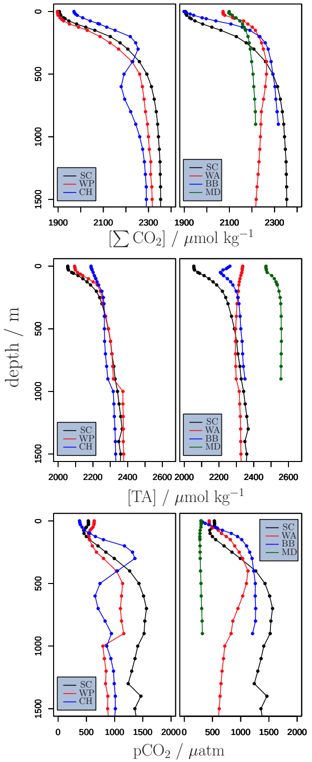

**Fig. 3.** Oceanographical data taken from Goyet et al. (2000) and limited to shallower depths when discontinuities occurred deeper. Top row: total dissolved inorganic carbon concentration [$\sum CO_2$]. Central row: total alkalinity concentration [TA]. Bottom row: carbon dioxide partial pressure $pCO_2$. (SC: Southern California (120.5° W, 29.50° N); CH: Chile (75.5° W, 33.5° S); WP: Western Pacific (126.5° E, 11.5° N), WA: Western Africa (6.5° E, 15.5° S), MD: Mediterranean (18.5° E, 35.5° N); BB: Bay of Bengal (87.5° E, 18.5° N)).

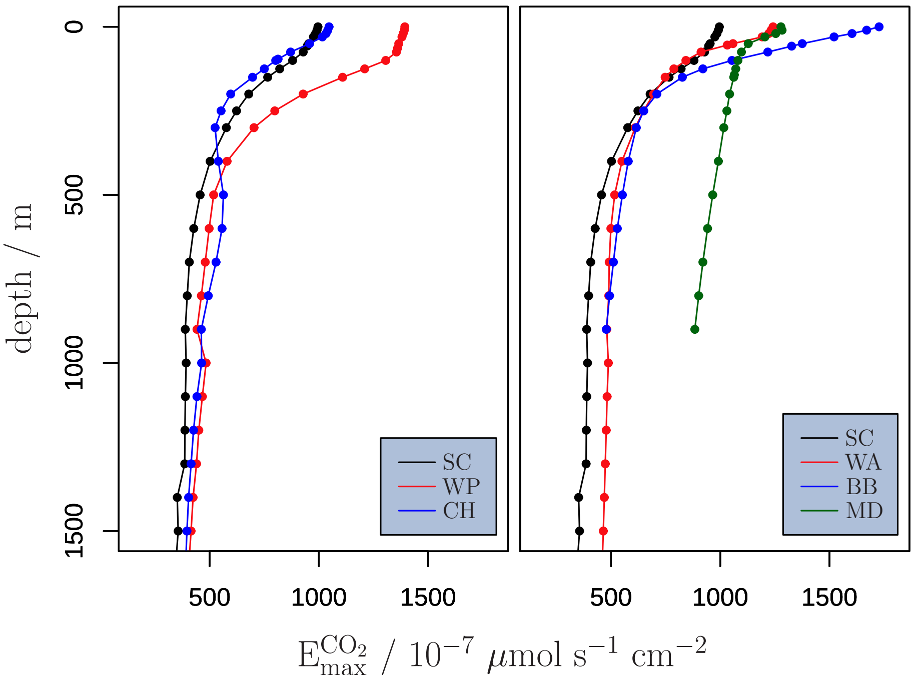

**Fig. 4.** Example depth profiles of the derived diffusive $CO_2$ export limitation quantity $E_{max}^{CO_2}$ (the maximal $CO_2$ diffusion limited metabolic rate). $pCO_2|_s^{max} = 5000$ µatm. Oceanographical data are taken from Goyet et al. (2000) and limited to shallower depths when discontinuities occurred deeper (SC: Southern California (120.5° W, 29.50° N); CH: Chile (75.5° W, 33.5° S); WP: Western Pacific (126.5° E, 11.5° N), WA: Western Africa (6.5° E, 15.5° S), MD: Mediterranean (18.5° E, 35.5° N); BB: Bay of Bengal (87.5° E, 18.5° N)).

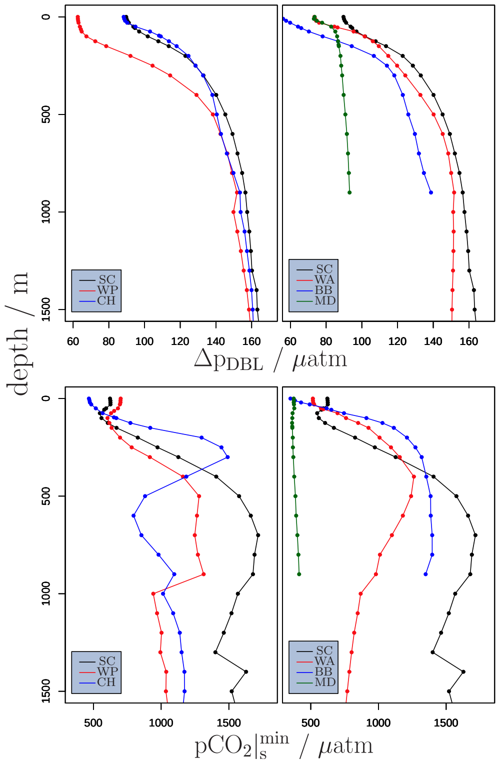

**Fig. 5.** Example depth profiles of the derived diffusive $CO_2$ export limitation quantities based on a given metabolic rate $E^{O_2} = 20 \times 10^{-7}$ µmol s$^{-1}$ cm$^{-2}$. Top panel: $\Delta p_{\mathrm{DBL}}$ (the minimal $CO_2$ partial pressure differential across the DBL required to sustain a given metabolic rate). Bottom panel: $p\mathrm{CO}_2|_s^{\min}$ (the minimal $CO_2$ partial pressure in molecular contact with a gas exchange surface that sustains a given metabolic rate under given external oceanic conditions). Oceanographical data are taken from Goyet et al. (2000) and limited to shallower depths when discontinuities occurred deeper (SC: Southern California (120.5° W, 29.50° N); CH: Chile (75.5° W, 33.5° S); WP: Western Pacific (126.5° E, 11.5° N), WA: Western Africa (6.5° E, 15.5° S), MD: Mediterranean (18.5° E, 35.5° N); BB: Bay of Bengal (87.5° E, 18.5° N)).

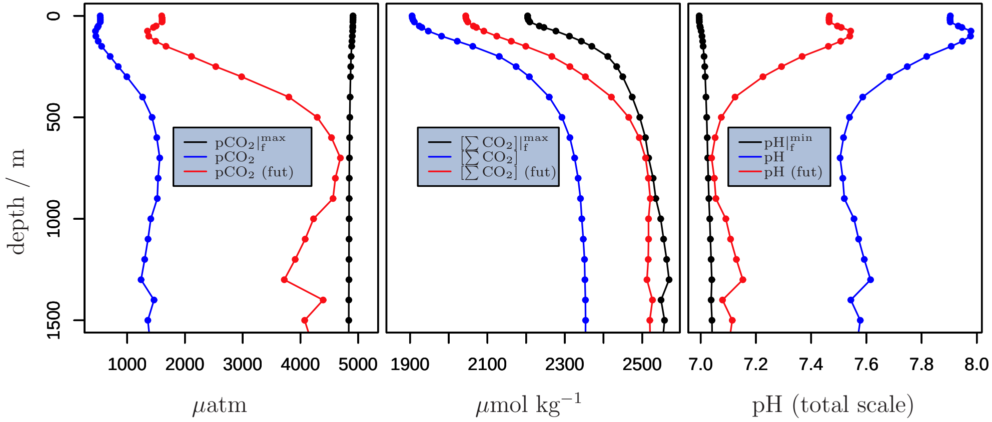

**Fig. 6.** Example depth profiles for the Southern California example station (SC, 120.5° W, 29.50° N) of limiting external conditions calculated based on derived diffusive $CO_2$ export limitation quantities assuming a given metabolic rate $E^{O_2} = 20 \times 10^{-7}$ µmol s$^{-1}$ cm$^{-2}$ and a given maximal $pCO_2$ in molecular contact with the gas exchange surface $pCO_2|_s^{max} = 5000$ µatm. Left panel: $pCO_2|_f^{max}$ (the maximal $CO_2$ partial pressure in the external bulk free stream that sustains a given metabolic rate; black line), compared to present-day ambient $pCO_2$ values (blue line) and assumed "future" $pCO_2$ values (red line, a tripled $pCO_2$ in the whole water column). Center panel: $[\sum CO_2]|_f^{max}$ (the maximal dissolved inorganic carbon concentration, as calculated from $pCO_2|_f^{max}$, sustaining a given metabolic rate; black line) compared to present-day $[\sum CO_2]$ values (blue line) and assumed "future" $[\sum CO_2]$ values (red line; consistent with a tripled $pCO_2$ in the whole water column). Right panel: $pH|_f^{min}$ (the minimal external total scale pH, as calculated from $pCO_2|_f^{max}$, sustaining a given metabolic rate; black line), compared to present-day total scale pH values (blue line), and assumed 'future" pH values (red line; consistent with a tripled $pCO_2$ in the whole water column). Oceanographical data are taken from Goyet et al. (2000).

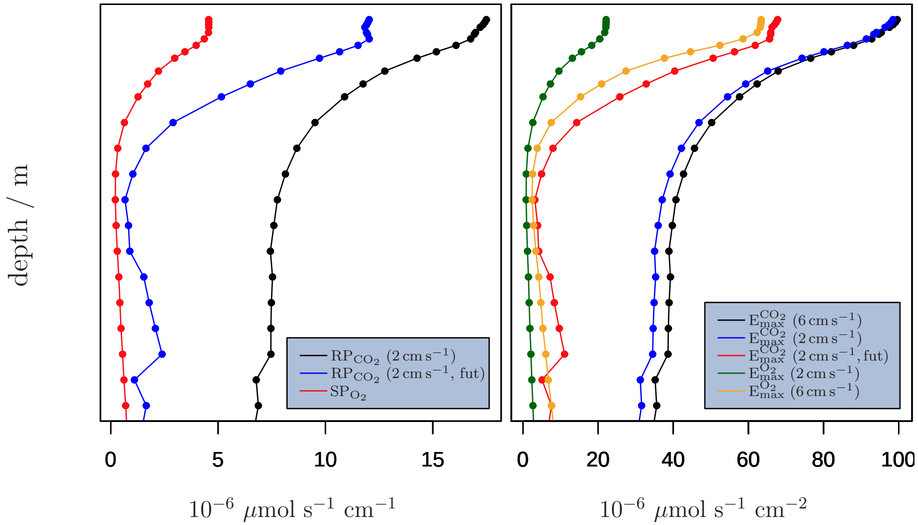

**Fig. 7.** Example depth profiles for the Southern California example station (SC, 120.5° W, 29.50° N) of diffusive carbon dixoide export limitation quantities as defined here, compared to equivalent diffusive oxygen uptake limitation quantities defined in the companion paper Hofmann et al. (2012). Left panel: $RP_{CO_2}$ (the oceanic $CO_2$ removal potential) calculated with $u_{100} = 2\,\mathrm{cm\,s^{-1}}$ and current ambient $p\mathrm{CO}_2$ values (black line) and assumed "future" tripled $p\mathrm{CO}_2$ values (blue line), compared to $SP_{O_2}$ (the oceanic oxygen supply potential, calculated according to Hofmann et al., 2012). Right panel: $E^{CO_2}_{max}$ (the maximal $CO_2$ diffusion limited metabolic rate), calculated with various given values for the fluid flow velocity $u_{100}$, and current and future $p\mathrm{CO}_2$ conditions, compared to $E^{O_2}_{max}$ (the maximal $O_2$ diffusion limited metabolic rate, calculated according to Hofmann et al. (2012) with various $u_{100}$ values and current oxygenation conditions). Oceanographical data for $CO_2$ are taken from the Goyet et al. (2000) climatology. Oceanographical data for $O_2$ are taken from the Garcia et al. (2010) oxygen climatology.

Title Page
Abstract
Introduction
Conclusions
References
Tables
Figures
◀◀
▶▶
◀
▶
Back
Close
Full Screen / Esc
Printer-friendly Version
Interactive Discussion